Hindawi
International Journal of Photoenergy
Volume 2021, Article ID 6692598, 10 pages
https://doi.org/10.1155/2021/6692598

*Research Article*

# On the Determination of the Output Power in Mono/Multicrystalline Photovoltaic Cells

**Xia Liu,[1] Yongqiu Liu,[1] and Mohammad Eslami[2]**

[1]*School of Electrical and Mechanical Engineering, Guangdong University of Science and Technology, Dongguan 523083, China*
[2]*Department of Electrical and Computer Engineering, Chabahar Branch, Islamic Azad University, Chabahar, Iran*

Correspondence should be addressed to Yongqiu Liu; banbianqiu@126.com and Mohammad Eslami; m.eslami@iauzah.ac.ir

Received 3 January 2021; Revised 11 February 2021; Accepted 17 April 2021; Published 8 May 2021

Academic Editor: Hafiz Muhammad Ali



In the present work, two artificial intelligence-based models were proposed to determine the output power of two types of photovoltaic cells including multicrystalline (multi-) and monocrystalline (mono-). Adaptive neuro-fuzzy inference system (ANFIS) and Least-squares support vector machine (LSSVM) are applied for the output power calculations. The estimation results are very close to the actual data based on graphical and statistical analysis. The coefficients of determination ($R^2$) of monocrystalline cell output power for LSSVM and ANFIS models are as 0.997 and 0.962, respectively. Additionally, multicells have $R^2$ values of 0.999 and 0.995 for LSSVM and ANFIS, respectively. The acceptable values for $R^2$ and various error parameters prove the accuracy of suggested models. The visualization of these comparisons clarifies the accuracy of suggested models. Additionally, the proposed models are compared with previously published machine learning methods. The accurate performance of proposed models in comparison with others showed that our models can be helpful tools for the estimation of output power. Moreover, a sensitivity analysis for the effects of inputs parameters on output power has been employed. The sensitivity output shows that light intensity has more on output power. The outcomes of this study provide interesting tools which have potential to apply in different parts of renewable energy industries.

## 1. Introduction

Photovoltaic (PV) cell power generation as a renewable energy source has vital importance, because it is not only used to overcome the present energy problems but also is environment-friendly to overcome the present environmental problems [1–3]. The development and studies in renewable energy technology can reduce the global warming problem and other environmental problems [4]. In the literature, there are some valuable studies on renewable energy topics such as experimental investigation on the effect on the mass flow rate of the nanofluid, volume fraction of the nanofluid, and volume of the storage tank on the inlet-outlet water temperature difference and the energy efficiency of an evacuated tube solar collector. Additionally, three machine learning approaches called gene-expression programming, model tree, and multivariate adaptive regression spline were developed for prediction of these target parameters [5]. Sadeghi et al. developed a modeling investigation on the evacuated tube solar collector. In their work, the gene-expression programming was used to simulate evacuated tube solar collector in various volumes of the thermal storage tanks and solar radiation intensities [6]. Akhter et al. evaluated the performance of three PV technologies including thin-film, monocrystalline, and poly-crystalline technologies based on eleven different performance parameters [7].

The device temperature and material and solar radiation intensity are effective parameters on the output power of PV cells. For instance, multicrystalline, monocrystalline, and amorphous crystalline silicon solar PV cells have different behaviors in the operational conditions. Therefore, an accurate predictive tool for determination of PV power supply and home power demand is highly required to save costs and time [8–10]. Among all predictive tools, the artificial intelligence (AI) approaches have a vital place for the determination of power because the AI approaches because of the ability of AI models in the prediction of the behavior of nonlinear dynamic systems [11]. In the AI approaches,

there is no need to employ any physics-based derivations or specific analytical formulations [12]. They do not require complex calculations or high amount of tuning parameters, and also, they have better performance than the multiple linear regression models in nonlinear systems [13, 14]. Overall, a dynamic system can be simulated by feeding a comprehensive dataset into an organized network. This network is trained until an acceptable degree of accuracy is obtained [15].

According to the successful background of intelligence methods in the prediction of different industrial parameters [16–18], in this work, two intelligence models based on adaptive neuro-fuzzy inference system (ANFIS) and Least-squares support vector machine (LSSVM) were suggested to determine the output power of two types of photovoltaic cells including multicrystalline and monocrystalline. Various comparisons have been carried out to investigate the performance of these models. Additionally, an interesting sensitivity analysis is employed to identify the impact of temperature and light intensity on output power.

## 2. Methodology

*2.1. Experimental Databank.* To train the aforementioned models, a comprehensive experimental databank was gathered from dependable sources in the literature. The experimental setup and conditions which were used to obtain these data points can be described as follows.

The utilized monocrystalline and multicrystalline PV cells have a size of 2.8 cm × 2.5 cm which was produced by QS Solar Company. For data acquisition, the PV testing system with number SAC which produced in Chengdu ZKY Instrument Company Xenon light source is used for the simulated sunlight. A six tranches toggle switch adjusts the intensity of the incident light. The light intensities of these tranches are around 1100, 1000, 900, 800, 700, and 600 W/m$^2$, respectively. A semiconductor refrigeration device was used for the temperature control room of an experimental sample.

The maximum output powers (MOP) and current-voltage curves were measured in temperatures of 40, 35, 30, 27, 25, 20, 15, 10, 5, 0, -5, and -10°C, respectively. Thus, each light intensity tranch has twelve measurement conditions. For instance, the experimental conditions of temperature and light intensity are -10°C and 6th tranche, -5°C and 6th tranche, 0°C and 6th tranche, 5°C and 6th tranche, 10°C and 6th tranche, 15°C and 6th tranche, 20°C and 6th tranche, 25°C and 6th tranche, 27°C and 6th tranche, 30°C and 6th tranche, 35°C and 6th tranche, and 40°C and 6th tranche. A total number of 72 actual points were collected, 62 of them were used as training data points, and 10 data points were used in the testing phase for evaluating the performance of models in unseen conditions [10].

*2.2. Adaptive Neuro-Fuzzy Inference System.* Fuzzy logic (FL) includes the inference strategy and cognitive uncertainties. On the other hand, artificial neural networks have parallel scattered structures which can be adapted quickly with different types of problems. Referring to these characteristics, the combination of these structures created neuro-fuzzy method. This method was employed by Takagi first time; after that, Jang proposed ANFIS. This model employed the abilities of both fuzzy and ANN structures to improve its performance [19]. In other words, this model combines fuzzy structure characteristic and adaptive system. The schematic structure of the ANFIS model is demonstrated in Figure 1. In this demonstration, fuzzy rules of the first-order Sugeno are expressed as follows: if $X_1 = A_i$ and $X_2 = B_j$ are acceptable, $f_i = m_i X_1 + n_i X_2 + r_i$ is assumed. In which, $r_i$, $m_i$, and $n_i$ are obtained in the process of training. The below figure gives information about the layered structure of this model [20]:

*Layer 1*: in this layer, adaptive nodes exist. These nodes can be considered as counterparts of linguistic terms, in which outputs have a relationship with membership function (MF) as follows:

$$O_i^1 = \beta(X) = \exp^{\left(-(1/2)\left((X-Z)^2/\sigma^2\right)\right)}. \quad (1)$$

In this formulation, $\sigma$, $Z$, and $O$ are the variances, Gaussian membership function center, and output, respectively.

*Layer 2*: this layer includes multiplying entrance signals to determine the fire strength:

$$O_i^2 = W_i = \beta_{Ai}(X).\beta_{Bi}(X). \quad (2)$$

*Layer 3*: this layer contains some firm nodes. The nodes determine the ratio of firing strength to the sum of all firing strength. The final outputs of this layer can be defined as follows:

$$O_i^3 = \frac{W_i}{\sum W_i}. \quad (3)$$

*Layer 4*: available adaptive nodes in this layer are used to calculate normalized firing strength as following:

$$O_i^4 = \overline{W}_i f_i = \overline{W}_i (m_i X_1 + n_i X_2 + r_i). \quad (4)$$

*Layer 5*: the final layer includes a node that sums the outputs of the fourth layer [21, 22]:

$$O_i^5 = Y = \sum_i \overline{W}_i f_i = \overline{W}_1 f_1 + \overline{W}_2 f_2 = \frac{\sum W_i f_i}{\sum W_i}. \quad (5)$$

*2.3. Least-Squares Support Vector Machine.* The cornerstone of support vector machine (SVM) is structural risk minimization and machine learning concepts. This algorithm can detect various patterns of available data and investigation of them based on a suitable way [23]. Seykens et al. upgraded SVM algorithm and called it least squares SVM (LSSVM). The significant point of the new algorithm is the fact that uses a linear equation system to solve the problem. This point makes it faster than the

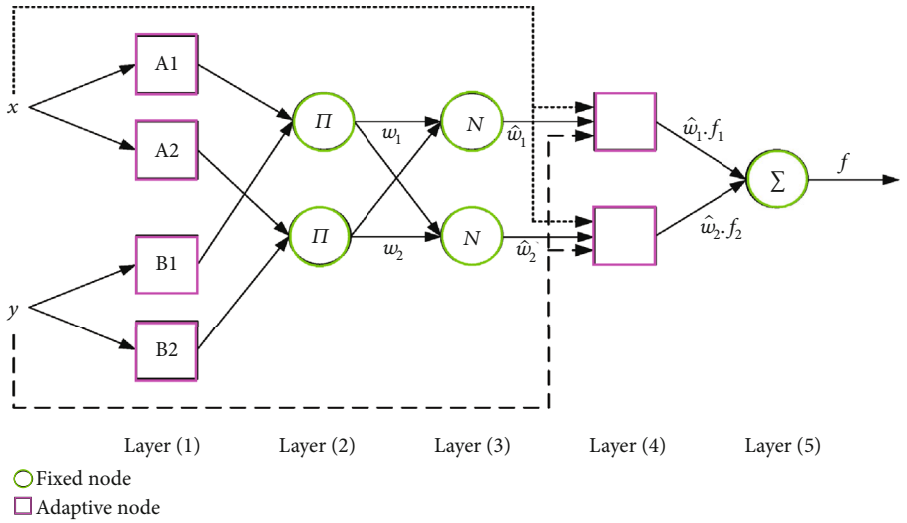


Figure 1: Structure of a typical ANFIS approach.

SVM algorithm. The below formulation describes the cost function of LSSVM method [24]:

$$\min_{\omega, b, e} J(\omega, e) = \frac{1}{2}\omega^T\omega + \frac{1}{2}\gamma\sum_{k=1}^{N} e_k^2. \quad (6)$$

The following constrain is defined for the cost function:

$$y_k = \omega^T\varphi(x_k) + b + e_k, k = 1, 2, \cdots, N. \quad (7)$$

In which, $b$ and $w$ are the bias and linear regression slope values, respectively. $\Upsilon$ stands for the regularization parameter. $x$ and $y$ stand for the input and output. $T$ and $\varphi$ are the transpose matrix and feature map. In the following, the Lagrange equation is defined:

$$L(\omega, b, e, \alpha) = J(\omega, e) - \sum_{k=1}^{N}\alpha_k\{\omega^T\varphi(x_k) + b + e_k - y_k\}. \quad (8)$$

In which, $\alpha_k$ is the Lagrangian multiplier which is estimated based on partial differentiation concept:

$$\begin{aligned}
&\frac{\partial L(\omega, b, e, \alpha)}{\partial\omega} = 0 \longrightarrow \omega = \sum_{k=1}^{N}\alpha_k\varphi(x_k),\\
&\frac{\partial L(\omega, b, e, \alpha)}{\partial b} = 0 \longrightarrow \sum_{k=1}^{N}\alpha_k = 0,\\
&\frac{\partial L(\omega, b, e, \alpha)}{\partial e_k} = 0 \longrightarrow \alpha_k = \gamma e_k, k = 1, 2, \cdots, N,\\
&\frac{\partial L(\omega, b, e, \alpha)}{\partial \alpha_k} = 0 \longrightarrow y_k = \omega^T\varphi(x_k) + b + e_k\, k = 1, 2, \cdots, N,
\end{aligned} \quad (9)$$

In which, $y = [y_1 \cdots y_N]^T$, $\alpha = [\alpha_1 \cdots \alpha_N]^T$, $1_N = [1 \cdots 1]^T$, and $I$ is the identity matrix. $\Omega_{kl}$ stands for $\varphi(x_k)^T\varphi(x_l) = K(x_k, x_l)$.

$$\begin{bmatrix} 0 & 1_v^T \\ 1_v & \Omega + \gamma^{-1}I \end{bmatrix}\begin{bmatrix} b \\ \alpha \end{bmatrix} = \begin{bmatrix} 0 \\ y \end{bmatrix}. \quad (10)$$

The LSSVM theory can be arranged in the other form:

$$y(x) = \sum_{k=1}^{N}\alpha_k K(x, x_k) + b. \quad (11)$$

In which, $K(x, x_k)$ is the kernel function that is in the form of radial basis function:

$$K(x_i, x_j) = e^{\left(-\left(\left(\|x_i - x_j\|^2\right)/\sigma^2\right)\right)}, \quad (12)$$

which $\sigma^2$ stands for radial basis width which is calculated during the training process. The process of determination of tuning parameters is shown in Figure 2[25]. The particle swarm optimization (PSO) is used for the determination of these parameters.

*2.4. Particle Swarm Optimization.* For the first time, the PSO algorithm was developed by Eberhart [26]. The main end of this approach is the determination of best conditions for nonlinear and complex problems. The motion of particles is the fundamental of finding global optimum in this method. Each particle stands for possible answers. During the optimization, the location and velocity of the particle are used. $g_{\text{best}}$ is known as the optimum solution from this algorithm, and $p_{\text{best}}$ is the best location of the particle in the defined domain. The below formulations

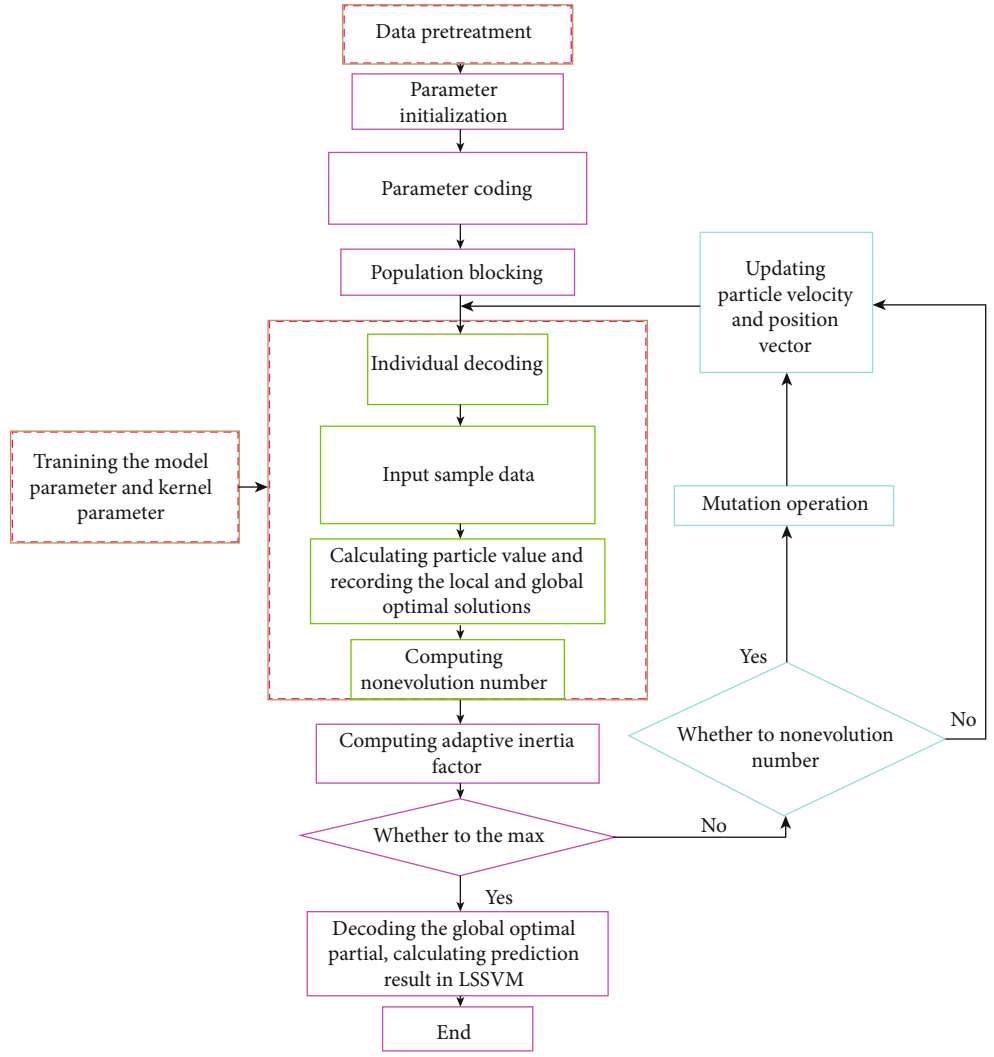


Figure 2: Structure LSSVM-PSO approach.

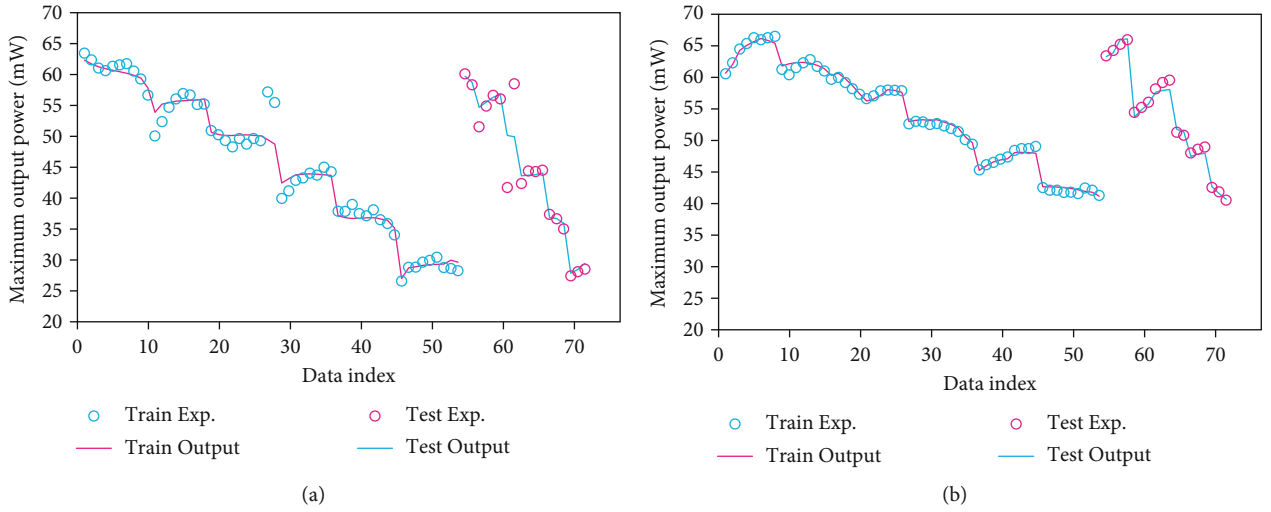


Figure 3: The predicted maximum output power by ANFIS for (a) monocells and (b) multicells.

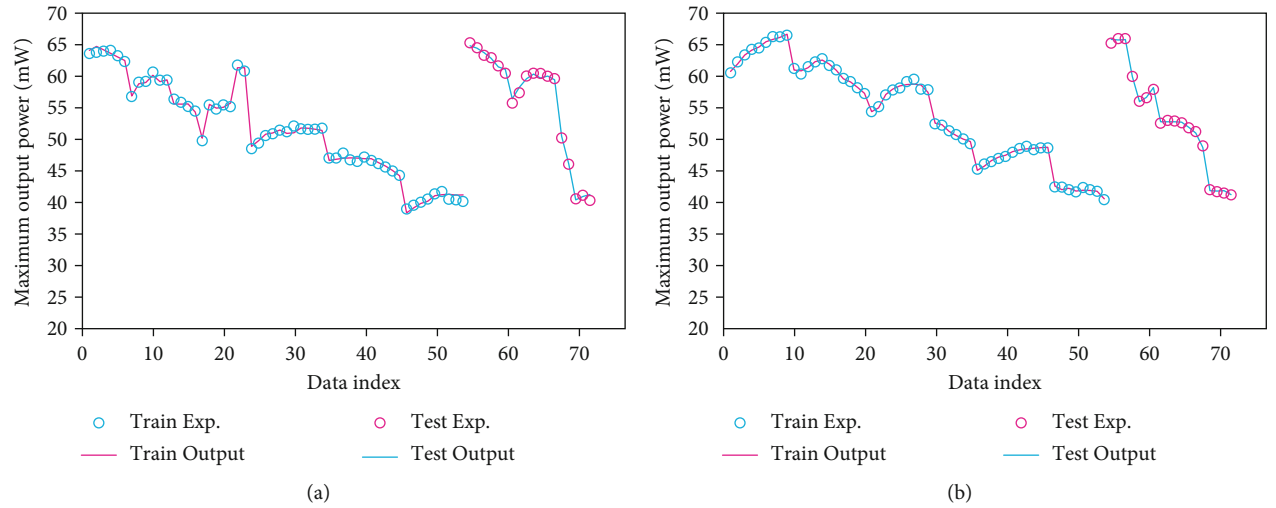


Figure 4: The predicted maximum output power by LSSVM for (a) monocells and (b) multicells.

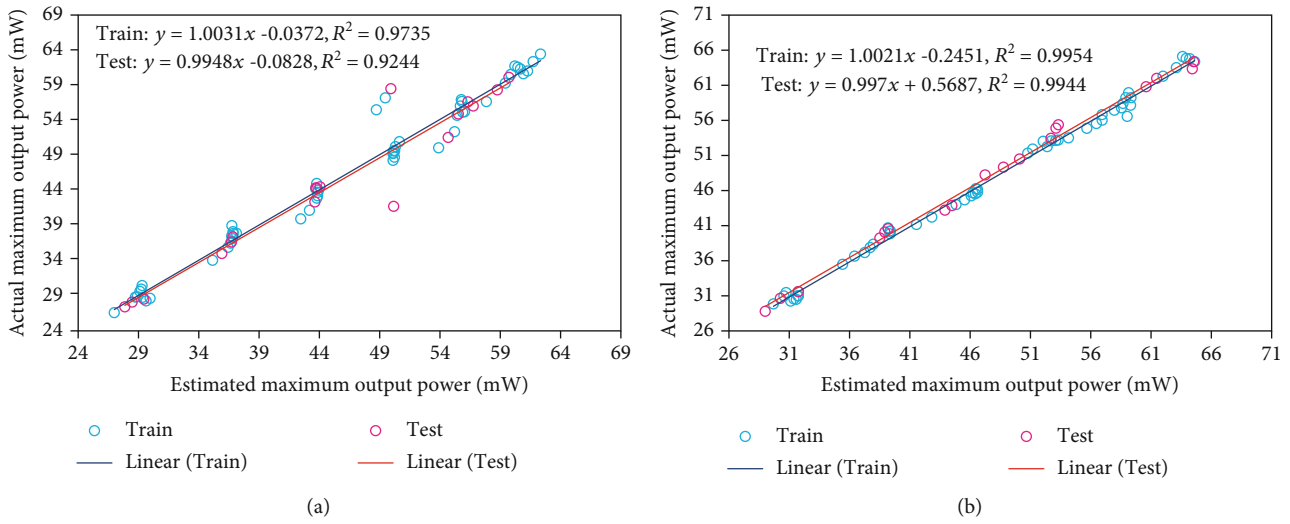


Figure 5: The cross plot of experimental and predicted maximum output power by ANFIS for (a) monocells and (b) multicells.

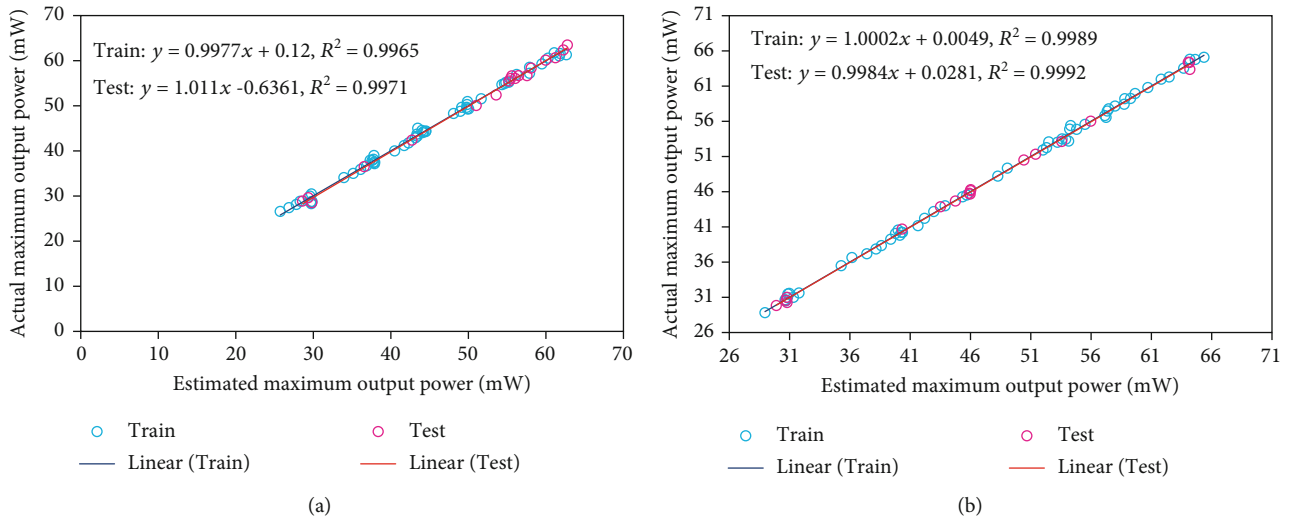


Figure 6: The cross plot of experimental and predicted maximum output power by LSSVM for (a) monocells and (b) multicells.

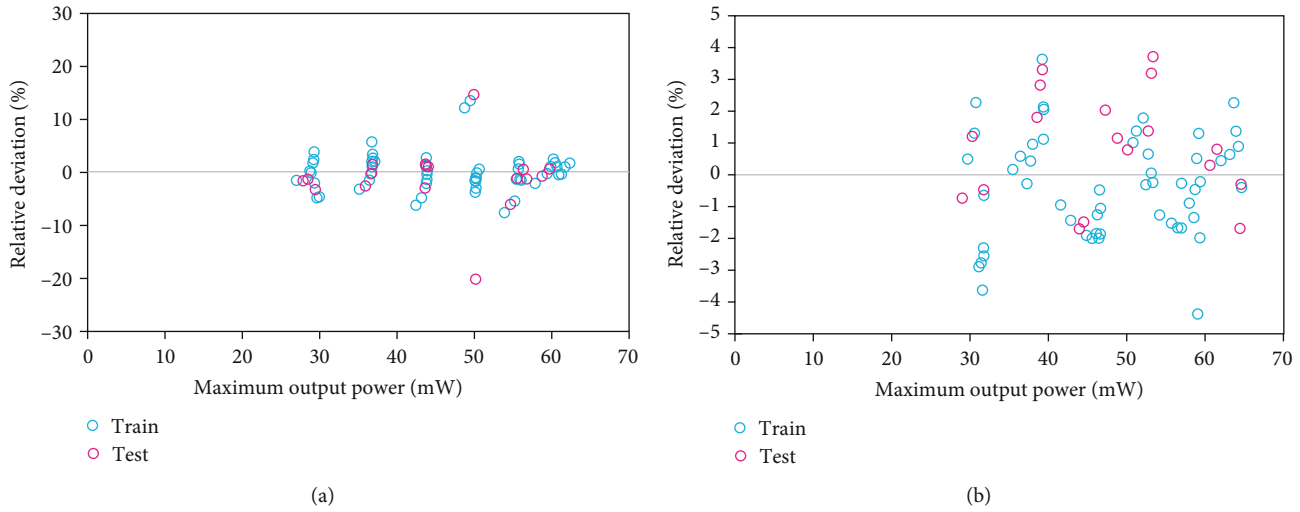


Figure 7: The relative deviation between experimental and predicted maximum output power by ANFIS for (a) monocells and (b) multicells.

show the ways that particle location and velocity are determined:

$$X_{\mathrm{pd}}^{\mathrm{iter}+1} = X_{\mathrm{pd}}^{\mathrm{iter}} + V_{\mathrm{pd}}^{\mathrm{iter}+1},$$

$$\begin{aligned} v_{\mathrm{id}}(t+1) = {} & w v_{\mathrm{id}}(t) + c_1 r_1 \left(p_{\mathrm{best,id}}(t) - X_{\mathrm{iid}}(t)\right) \\ & + c_2 r_2 \left(g_{\mathrm{best},d}(t) - X_{\mathrm{id}}(t)\right). \end{aligned} \tag{13}$$

$Vi(t)$ and $Xi(t)$ stand for the velocity and position of the particle, respectively. $c_1$ and $c_2$ show the learning terms which can control the speed of the particle. $w$ is used as a connection between previous velocity and current value. $r_1$ and $r_2$ are random values between 0 and 1 [27, 28]. There are other optimization algorithms in the literature. Genetic algorithm (GA) and hybrid of GA and PSO (HGAPSO) are well-known algorithms which can be used for optimization of LSSVM and ANFIS algorithms. Their combinations with these predictive tools create great models for the prediction of different processes in the industries [24, 25].

## 3. Results and Discussion

In the present part, the outputs of models and experimental output powers for these two types of cells are compared to ensure the accuracy and ability of models. To this end, graphical and statistical comparisons are carried. First, for graphical comparison, the simultaneous illustrations of predicted and actual output power for monocells and multicells are shown in Figures 3 and 4 for ANFIS and LSSVM models, respectively. These comparisons show that models outputs have an agreement with experimental values.

The cross plots for these models are depicted in Figures 5 and 6. The regression lines for monocells and multicells show that they have similar equations to $y = x$ line. The coefficients of determination parameters for these lines are near one. Therefore, the accuracy of proposed models in the determination of output power is acceptable. The details of discussing lines are shown in Figures 5 and 6. The compaction of output power data points near the bisector shows that models have enough accuracy in the determination of output power.

The relative deviation between predicted and experimental values for ANFIS and LSSVM models is shown in Figures 7 and 8. The concentration of relative deviations around the $x$-axis line shows that the proposed models have great accuracy in the wide range of output powers. As a noticeable point, the trained models have better accuracy in the prediction of output power values for multicells. The best performance belongs to the LSSVM algorithm for the prediction of multicell with a relative error lower than 2 percent.

The coefficients of determination ($R^2$), mean relative error (MRE), mean squared errors (MSEs), relative mean squared errors (RMSEs), and Standard deviations (STDs) are formulated as below [29–31]:

$$\begin{aligned} R^2 &= 1 - \frac{\sum_{i=1}^{N} \left(X_i^{\mathrm{actual}} - X_i^{\mathrm{predicted}}\right)^2}{\sum_{i=1}^{N} \left(X_i^{\mathrm{actual}} - \bar{X}^{\mathrm{actual}}\right)^2}, \\ \mathrm{MRE} &= \frac{100}{N} \sum_{i=1}^{N} \left| X_i^{\mathrm{predicted}} - X_i^{\mathrm{actual}} \right|, \\ \mathrm{MSE} &= \frac{100}{N} \sum_{i=1}^{N} \left(X_i^{\mathrm{actual}} - X_i^{\mathrm{predicted}}\right)^2, \\ \mathrm{RMSE} &= \sqrt{\frac{100}{N} \sum_{i=1}^{N} \left(X_i^{\mathrm{actual}} - X_i^{\mathrm{predicted}}\right)^2}, \\ \mathrm{STD}_{\mathrm{error}} &= \left( \frac{1}{N-1} \sum_{i=1}^{N} (\mathrm{error} - \overline{\mathrm{error}}) \right)^{0.5}. \end{aligned} \tag{14}$$

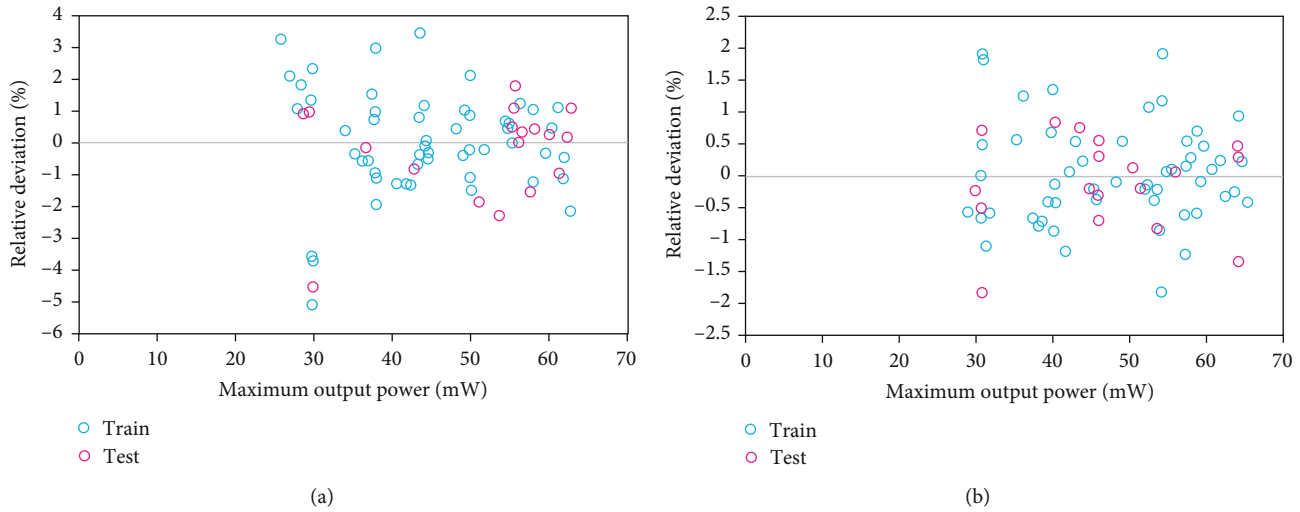


Figure 8: The relative deviation between experimental and predicted maximum output power by LSSVM for (a) monocells and (b) multicells.

Table 1: Statistical evaluations of models.

| | | | $R^2$ | MRE (%) | MSE | RMSE | STD |
|---|---|---|---|---|---|---|---|
| Monocell | LSSVM | Train | 0.997 | 1.232 | 0.37366882 | 0.6113 | 0.3621 |
| | | Test | 0.997 | 1.097 | 0.413593905 | 0.6431 | 0.4053 |
| | | Total | 0.997 | 1.198 | 0.383650091 | 0.6431 | 0.3705 |
| Multicell | | Train | 0.999 | 0.617 | 0.131896651 | 0.3632 | 0.2304 |
| | | Test | 0.999 | 0.570 | 0.104762187 | 0.3237 | 0.2049 |
| | | Total | 0.999 | 0.605 | 0.125113035 | 0.3237 | 0.2232 |
| Monocell | ANFIS | Train | 0.973 | 2.496 | 3.282398807 | 1.8117 | 1.4126 |
| | | Test | 0.924 | 3.460 | 8.918576686 | 2.9864 | 2.5967 |
| | | Total | 0.962 | 2.737 | 4.691443277 | 2.9864 | 1.7726 |
| Multicell | | Train | 0.995 | 1.370 | 0.573499732 | 0.7573 | 0.4360 |
| | | Test | 0.994 | 1.603 | 0.860051592 | 0.9274 | 0.5437 |
| | | Total | 0.995 | 1.428 | 0.645137697 | 0.9274 | 0.4652 |

Determination of above parameters shows the accuracy of models in the prediction of the output power of photovoltaic cells. The calculated parameters are inserted in Table 1.

As can be seen, the LSSVM model has better accuracy in comparison with the ANFIS model. The determined $R^2$ values for monocell and multicell are 0.997 and 0.999 for LSSVM, respectively. The calculated $R^2$ values of ANFIS model are reported 0.962 and 0.995 for monocell and multicell, respectively. Moreover, the MSE values of LSSVM are 0.3836 and 0.1251 for monocell and multicell, respectively. The MSE values of 4.6914 and 0.6451 are reported for monocell and multicell, respectively. Furthermore, the other error parameters are very low for the LSSVM model. Therefore, the accuracy and performance of this algorithm are acceptable for the estimation of the output power of photovoltaic cells. Xiao et al. used the different structure of ANN algorithms for the estimation of output power. The best predictive structures for their work had 8 and 9 hidden layer unit with an average correlation coefficient of 0.97 and 0.988 for monocrystalline and multicrystalline. Our proposed models have better performance than these ANN-based methods [10].

One of the well-known analyses which are carried in this study is the estimation of the relevancy factor for inputs. The relevancy factor describes the impacts of the considered input parameter on the output power of photovoltaic cells. This factor can be formulated as below [25, 32]:

$$r = \frac{\sum_{i=1}^{n}\left(X_{k,i} - \overline{X_k}\right)\left(Y_i - \bar{Y}\right)}{\sqrt{\sum_{i=1}^{n}\left(X_{k,i} - \overline{X_k}\right)^2 \sum_{i=1}^{n}\left(Y_i - \bar{Y}\right)^2}}. \quad (15)$$

Herein, $Y_i$, $\bar{Y}$, $X_{k,i}$, and $\overline{X_k}$ stand for the "$i$" th output, output average, $k$th of input, and average of inputs [21]. The estimated relevancy factor for each input is demonstrated in Figure 9 which shows that the most effective parameter on the output power of cells is light intensity with $r$ value of

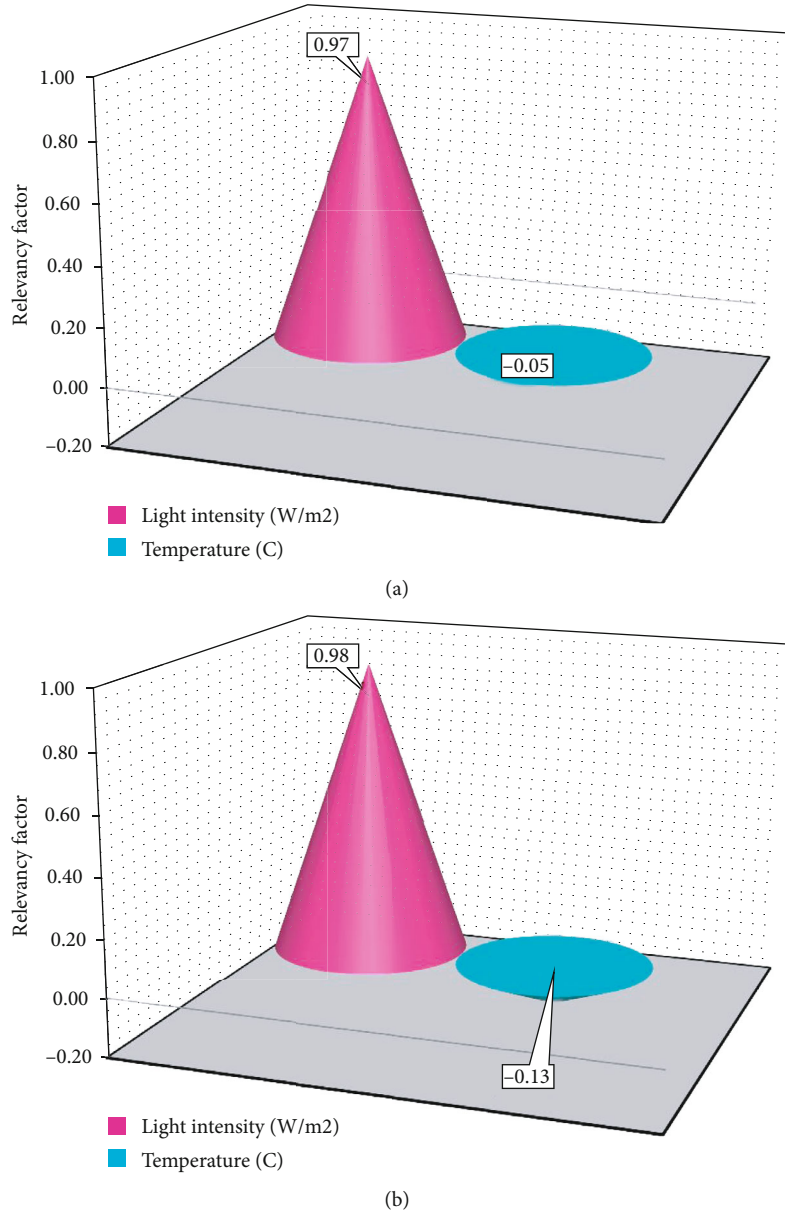


Figure 9: Impacts of input parameters on output power of (a) monocells and (b) multicells.

0.97. Additionally, the values of output power will increase if light intensity increases. On the other hand, the negative values of the relevancy factor for temperature show that there is a reverse relationship between temperature and output power.

## 4. Conclusions

In this work, two artificial intelligence methods based on ANFIS-PSO and LSSVM-PSO have been developed to determine the output power of two types of photovoltaic cells. The employed models show great accuracy in graphical and statistical comparisons. The coefficients of determination ($R^2$) of monocrystalline cell output power for LSSVM and ANFIS models are determined as 0.997 and 0.962, respectively. Additionally, multicells have $R^2$ values of 0.999 and 0.995 for LSSVM and ANFIS, respectively. The lower error values show that the present models have great accuracy in the prediction of cell output power. The graphical comparisons are also employed to the better demonstration of agreement between predicted and actual output power values. After that, a sensitivity analysis has been carried out to show the relationship of input parameters and output power of these cells. According to the obtained results, the present work provides useful information about the determination of output power for different types of cells. The suggested models can determine this parameter by consuming the least time and cost. The main limitation of these methods is that they need a comprehensive dataset for training models and obtaining tuning parameters. If a limited number of experimental data points are used in the training phase, the performance of the model in determination of unseen conditions will be limited.

According to this fact, a comprehensive and large experimental databank which covers a wide range of operational conditions should be provided.

## Data Availability

The data that support the findings of this study are available from the corresponding author, upon reasonable request.

## Conflicts of Interest

The authors declare no conflicts of interest.

## Acknowledgments

The study is financially supported by the Key research project of Guangdong University of Science & Technology in 2020: Algorithm Research on smart Grid Power Supply Restoration (GKY-2020KYZDK-3).

## References

[1] X. Hu, Y. Zou, and Y. Yang, "Greener plug-in hybrid electric vehicles incorporating renewable energy and rapid system optimization," *Energy*, vol. 111, pp. 971–980, 2016.

[2] J.-T. Liu, X.-H. Deng, W. Yang, and J. Li, "Perfect light trapping in nanoscale thickness semiconductor films with a resonant back reflector and spectrum-splitting structures," *Physical Chemistry Chemical Physics*, vol. 17, no. 5, pp. 3303–3308, 2015.

[3] G. K. Singh, "Solar power generation by PV (photovoltaic) technology: a review," *Energy*, vol. 53, pp. 1–13, 2013.

[4] M. N. Akhter, S. Mekhilef, H. Mokhlis, and N. M. Shah, "Review on forecasting of photovoltaic power generation based on machine learning and metaheuristic techniques," *IET Renewable Power Generation*, vol. 13, no. 7, pp. 1009–1023, 2019.

[5] G. Sadeghi, M. Najafzadeh, and M. Ameri, "Thermal characteristics of evacuated tube solar collectors with coil inside: an experimental study and evolutionary algorithms," *Renewable Energy*, vol. 151, pp. 575–588, 2020.

[6] G. Sadeghi, M. Najafzadeh, and H. Safarzadeh, "Utilizing gene-expression programming in modelling the thermal performance of evacuated tube solar collectors," *Journal of Energy Storage*, vol. 30, p. 101546, 2020.

[7] M. N. Akhter, S. Mekhilef, H. Mokhlis, L. Olatomiwa, and M. A. Muhammad, "Performance assessment of three grid-connected photovoltaic systems with combined capacity of 6.575 $kW_p$ in Malaysia," *Journal of Cleaner Production*, vol. 277, 2020.

[8] K. Gajowniczek and T. Ząbkowski, "Electricity forecasting on the individual household level enhanced based on activity patterns," *PLoS One*, vol. 12, no. 4, 2017.

[9] X. Wu, X. Hu, S. Moura, X. Yin, and V. Pickert, "Stochastic control of smart home energy management with plug-in electric vehicle battery energy storage and photovoltaic array," *Journal of Power Sources*, vol. 333, pp. 203–212, 2016.

[10] W. Xiao, G. Nazario, H. Wu, H. Zhang, and F. Cheng, "A neural network based computational model to predict the output power of different types of photovoltaic cells," *PLoS One*, vol. 12, no. 9, 2017.

[11] A. Mellit and S. A. Kalogirou, "Artificial intelligence techniques for photovoltaic applications: a review," *Progress in Energy and Combustion Science*, vol. 34, no. 5, pp. 574–632, 2008.

[12] Z. Lei, W. Zhenpo, H. Xiaosong, and D. G. Dorrell, "Residual capacity estimation for ultracapacitors in electric vehicles using artificial neural network," *IFAC Proceedings Volumes*, vol. 47, no. 3, pp. 3899–3904, 2014.

[13] D. A. Fadare, "Modelling of solar energy potential in Nigeria using an artificial neural network model," *Applied Energy*, vol. 86, no. 9, pp. 1410–1422, 2009.

[14] E. Izgi, A. Öztopal, B. Yerli, M. K. Kaymak, and A. D. Şahin, "Short–mid-term solar power prediction by using artificial neural networks," *Solar Energy*, vol. 86, no. 2, pp. 725–733, 2012.

[15] E. F. Fernández, F. Almonacid, N. Sarmah, P. Rodrigo, T. K. Mallick, and P. Pérez-Higueras, "A model based on artificial neuronal network for the prediction of the maximum power of a low concentration photovoltaic module for building integration," *Solar Energy*, vol. 100, pp. 148–158, 2014.

[16] M. Najafzadeh and H. M. Azamathulla, "Neuro-fuzzy GMDH to predict the scour pile groups due to waves," *Journal of Computing in Civil Engineering*, vol. 29, no. 5, 2015.

[17] M. Najafzadeh, A. Etemad-Shahidi, and S. Y. Lim, "Scour prediction in long contractions using ANFIS and SVM," *Ocean Engineering*, vol. 111, pp. 128–135, 2016.

[18] M. Najafzadeh and A. Zahiri, "Neuro-fuzzy GMDH-based evolutionary algorithms to predict flow discharge in straight compound channels," *Journal of Hydrologic Engineering*, vol. 20, no. 12, 2015.

[19] J.-S. R. Jang, C.-T. Sun, and E. Mizutani, "Neuro-fuzzy and soft computing-a computational approach to learning and machine intelligence [book review]," *IEEE Transactions on Automatic Control*, vol. 42, no. 10, pp. 1482–1484, 1997.

[20] J.-S. R. Jang, "ANFIS: adaptive-network-based fuzzy inference system," *IEEE Transactions on Systems, Man, and Cybernetics*, vol. 23, no. 3, pp. 665–685, 1993.

[21] A. Bemani, A. Baghban, and A. H. Mohammadi, "An insight into the modeling of sulfur content of sour gases in supercritical region," *Journal of Petroleum Science and Engineering*, vol. 184, p. 106459, 2020.

[22] R. Daneshfar, A. Bemani, M. Hadipoor et al., "Estimating the heat capacity of non-Newtonian ionanofluid systems using ANN, ANFIS, and SGB tree algorithms," *Applied Sciences*, vol. 10, no. 18, p. 6432, 2020.

[23] K. Pelckmans, J. A. Suykens, T. Van Gestel et al., "LS-SVMlab: a matlab/c toolbox for least squares support vector machines," in *Tutorial*, KULeuven-ESAT, Leuven, Belgium, 2002.

[24] A. Bemani, Q. Xiong, A. Baghban, S. Habibzadeh, A. H. Mohammadi, and M. H. Doranehgard, "Modeling of cetane number of biodiesel from fatty acid methyl ester (FAME) information using GA-, PSO-, and HGAPSO- LSSVM models," *Renewable Energy*, vol. 150, pp. 924–934, 2020.

[25] R. Razavi, A. Bemani, A. Baghban, and A. H. Mohammadi, "Modeling ofCO2absorption capabilities of amino acid solutions using a computational scheme," *Environmental Progress & Sustainable Energy*, vol. 39, no. 6, 2020.

[26] R. Eberhart and J. Kennedy, "A new optimizer using particle swarm theory, MHS'95," *Proceedings of the Sixth International Symposium on Micro Machine and Human Science*, 1995, pp. 39–43, Nagoya, Japan, 1995.

[27] J.-S. Chiou, S.-H. Tsai, and M.-T. Liu, "A PSO-based adaptive fuzzy PID-controllers," *Simulation Modelling Practice and Theory*, vol. 26, pp. 49–59, 2012.

[28] Y. Shi and R. Eberhart, "A modified particle swarm optimizer," in *1998 IEEE International Conference on Evolutionary Computation Proceedings. IEEE World Congress on Computational Intelligence (Cat. No.98TH8360)*, pp. 69–73, Anchorage, AK, USA, 1998.

[29] M. Najafzadeh and F. Saberi-Movahed, "GMDH-GEP to predict free span expansion rates below pipelines under waves," *Marine Georesources & Geotechnology*, vol. 37, no. 3, pp. 375–392, 2019.

[30] M. Najafzadeh, F. Saberi-Movahed, and S. Sarkamaryan, "NF-GMDH-based self-organized systems to predict bridge pier scour depth under debris flow effects," *Marine Georesources & Geotechnology*, vol. 36, no. 5, pp. 589–602, 2018.

[31] F. Saberi-Movahed, M. Najafzadeh, and A. Mehrpooya, "Receiving more accurate predictions for longitudinal dispersion coefficients in water pipelines: training group method of data handling using extreme learning machine conceptions," *Water Resources Management*, vol. 34, no. 2, pp. 529–561, 2020.

[32] E. Khamehchi and A. Bemani, "Prediction of pressure in different two-phase flow conditions: machine learning applications," *Measurement*, vol. 173, 2021.